DETERMINING THE WATER CONTENT OF ANCIENT LUNAR BASALTS FROM VOLATILES IN APATITE AND SILICATE MINERALS. Katharine L. Robinson [1,2,*], Kazuhide Nagashima[3], Barry J. Shaulis[4], Gary R. Huss[3], G. Jeffrey Taylor[3], and David A. Kring[1,2] [1]CLSE, LPI/USRA, 3600 Bay Area Blvd., Houston, TX 77058, [2]NASA SSERVI [3]HIGP, Univ. Hawai'i at Mānoa, 1680 East-West Rd., Honolulu HI 96822. [4]TraIL, Univ. of Arkansas, Fayetteville, AR 72701. *robinson@lpi.usra.edu

Introduction: A key goal of volatile measurements in lunar samples is to determine the initial volatile compositions and abundances of their parental magmas. Lunar basalts are particularly important as they form through partial melting of the lunar mantle, and can provide information about volatiles in their respective mantle sources. Most sample-based studies of volatiles in lunar rocks have focused on the common accessory mineral apatite [$Ca_5(PO_4)_3(OH,F,Cl)$] (e.g., [1,2]). Apatite can preserve information about volatile abundance and isotopic composition, but it can only be used to infer magmatic volatile abundances in specific compositional circumstances [3,4]. Measurements of lunar pyroclastic glasses [5] and melt inclusions [6,7] avoid this issue, but these are relatively rare in the lunar sample collection.

Common nominally anhydrous minerals (NAMs) such as olivine, plagioclase, and pyroxene, can contain small amounts of volatiles. Volatiles enter these minerals according to simple partitioning coefficients [3,8]. We developed a technique using secondary ion mass spectrometry (SIMS) to measure volatiles in NAMs. Here, we present the first coordinated measurements of volatiles in silicates and apatite (reported in Robinson et al. [9]) in the same lunar sample.

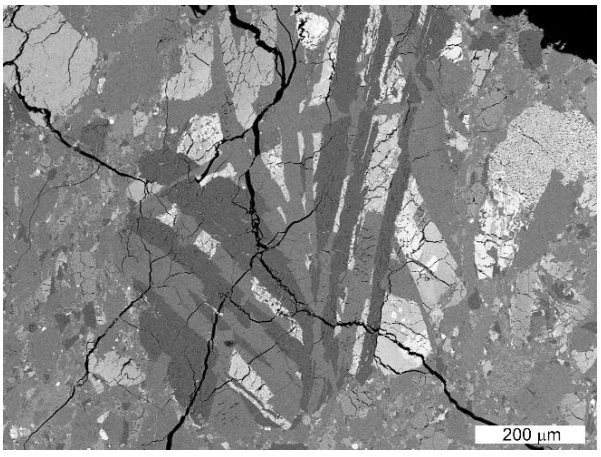

Fig.1. Backscattered electron image of a representative basaltic fragment in MIL 13317,23.

Sample: Miller Range (MIL) 13317 is a feldspathic lunar breccia containing numerous low-Ti basaltic fragments (Fig. 1) [11-13]. These basalts represent some of the oldest known volcanism on the Moon (~4.332 Ga) and are, therefore, ideal samples for examining the role of volatiles early in lunar history [9-12]. We studied two thin sections of MIL 13317: -,5 and -,23. Several of the basalt fragments contain apatite in incompatible-element rich mesostasis areas (Fig. 2), often coexisting with products of pyroxferroite breakdown (fayalite, Fe-rich pyroxene, silica) [9,10,13]. All basaltic fragments show evidence of shock; plagioclase has been largely converted to maskelynite in all of the measured fragments and the mafic minerals are badly fractured [10].

Methods: Plagioclase and pyroxene in MIL 13317 were analyzed with a ~5 nA primary Cs+ beam defocused to ~30 μm (Fig. 2). Data collection was restricted with a field aperture to the inner ~4 μm of the spot. We measured $^{12}C^-$, $^{16}O^1H^-$, $^{18}O^-$ $^{19}F^-$, $^{30}Si^-$, $^{31}P^-$, $^{32}S^-$, and $^{35}Cl^-$ ions sequentially using an electron multiplier. Mass resolving power was set to ~5400, sufficient to resolve all species from interfering ions. Abundances were calculated with (species)/^{30}Si versus wt.% (species) calibration curves constructed for each ion using terrestrial basaltic and rhyolitic glasses (FJ-G2, MRN-G1 [14]) and orthopyroxene (SLP-142 [15]; NMNH 116610-5 [16]). The curves were forced through the origin. Uncertainties on the slopes range from 2 to 6% (2σ). The reported uncertainty includes 2-SE from individual measurements convolved with a fixed 10% relative error. Instrumental background was determined to be ~5 ppm H_2O based on repeated measurements of Suprasil 3002 (<1 ppm H_2O). Background H_2O was subtracted from the calculated H_2O abundances of the unknowns.

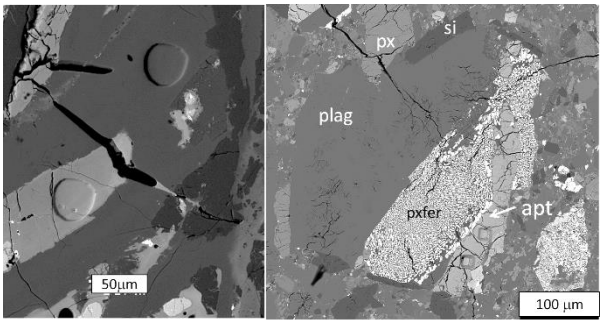

Fig. 2. SIMS analysis pits in pyroxene and plagioclase in a basaltic fragment (left) and in apatite from Clast 2 (right, from [9]).

Results and Implications: We obtained 12 plagioclase measurements from 7 different clasts. Plagioclase in MIL 13317 contains <1 to ~41±5 ppm H_2O. A few

plagioclase and all pyroxene measurements were discarded due to contamination by epoxy-filled cracks near the measured area. Our previous measurements show apatite in MIL 13317 basalt fragments is highly enriched in ^{37}Cl, with $\delta^{37}Cl$ of 29 to 36‰ [9,10]. The single apatite grain large enough to be measured for D/H (Fig. 2) contains ~2000 ppm H_2O and has δD of ~ +650‰ [9,10].

We measured the volatile content of plagioclase coexisting with apatite in Clast 2, which is thought to be a fragment of mesostasis broken from a larger basaltic fragment [9,10]. We can then calculate the water abundance of the clast's parental melt using both the NAM and the apatite's water content. Because these phases crystallized from the same parental melt, they serve as a self-check for the calculation.

The H_2O content of a melt at the time of mineral crystallization is calculated using H_2O mineral-melt partition coefficients ($D_{min\text{-}H2O}$). The $D_{plag\text{-}H2O}$ is somewhat dependent on the fO_2 of the melt (e.g., [17]). Lunar basalts formed under reduced conditions so we use $D_{plag\text{-}H2O}$ = 0.018 – 0.046, determined from experiments done at iron-wustite [17,18]. Plagioclase in this clast contains ~8 ppm H_2O, which corresponds to a melt H_2O of 170 to 440 ppm at the time of plagioclase crystallization.

Partition coefficients for F, Cl, and OH into apatite are highly variable [3,4,19]. Exchange coefficients (K_d), ratios of distribution coefficients relative to each other, are much less variable for apatite [4,19]. However, the melt F or Cl content must be known and the apatite must fall into a certain compositional range ([4,19]; Fig. 3). Using Eq. 8 from McCubbin et al [4]:

$$X_{H2O}^{pm} = \frac{X_{H2O}^{Ap} \times X_F^{pm}}{K_d{}_{OH-F}^{Ap-melt} \times X_F^{Ap}}$$

where X_{H2O}^{PM} is the H_2O content of the parent melt, X_{H2O}^{Ap} is the apatite H_2O content, X_F^{PM} is the parent melt F content, $K_d{}_{OH-F}^{Ap-Melt}$ = 0.014 [4], and X_F^{Ap} is the F abundance of the apatite, we can calculate the abundance of water in the apatite's parental melt.

Parent melt F is estimated with F abundance in plagioclase and its partition coefficient [18], or from the F content of Apollo picritic glasses [5]. Taking 5 to 72 ppm F in the parent melt based on the F content of MIL 13317 plagioclase and Apollo glasses [5], and using the abundance of F measured in MIL 13317 apatite 2, we estimate the parent melt of MIL 13317 basalt contained 28 to 575 ppm H_2O. The range determined from apatite is consistent with the range of possible melt H_2O abundances determined from H_2O partitioning into coexisting plagioclase (170 to 440 ppm H_2O). While these estimates have substantial uncertainties due to uncertainties in the partition coefficients and parental melt F content, the fact that they are internally consistent *and* consistent with previously reported H_2O contents of lunar mare basalts [5,6] suggests they are valid estimates. Other clasts in MIL 13317 have <1 to 41 ppm H_2O (which yield estimated H_2O contents from 24 to 2280 ppm). It is not clear why the plagioclase is so much more water-rich in these clasts versus Clast 2. If the highest-water plagioclase is in fact representative of the parental basaltic melt, the magma contained <0.23 wt.% H_2O and was still extremely dry compared with all but the driest terrestrial magmas [5,6,20].

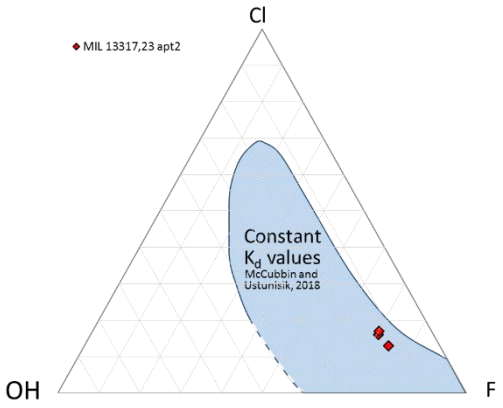

Fig. 3. Apatite X-site ternary diagram showing the composition of MIL 13317,23 Apatite 2. Apatite with compositions that fall within the shaded area may be used for apatite hygrometry [19].

References: [1] Boyce J.W. et al. (2010*) Nature, 466*, 466–469. [2] McCubbin F.M. et al. (2010) *PNAS, 107*,11223–11228. [3] Boyce J.W. (2014) *Science Express*, 10.1126/science.1250398 [4] McCubbin F.M. et al. (2015) *Amer. Min., 100*, 1790–1802. [5] Saal A.E. et al. (2008) *Nature, 454*, 192–195. [6] Hauri E.H. et al. (2011) *Science, 333*, 213–215. [7] Saal A.E. et al. (2013) *Science, 340*, 1317–1320. [8] Hamada M. et al. (2013) *EPSL, 365*, 253–262. [9] Robinson K.L. et al. (2019) *LPS L*, abs.# 2063. [10] Robinson K.L et al. (2019), in review at *EPSL*. [11] Shaulis B.J. et al. (2016) *LPS XLVII*, abs.#2027 [12] Snape J.F. et al. (2018) *EPSL 502*, 84–95. [13] Curran N.M. et al. (2019) *MaPS, 54*, 1401–1430 [14] Shimizu K. et al. (2017) *Geochem. J.*, 51, 299–313. [15] Peslier A.H. et al. (2002) *EPSL, 201*, 69–86. [16] Kumamoto K.M. et al. (2017) *Amer. Min., 102*, 537–547. [17] Lin Y. et al. (2019) *Geochem. Pers. Lett., 10*, 14–19. [18] Caseres J.R., et al. (2017) *LPS XLVIII*, abs. #2303 [19] McCubbin F.M., Ustunisik G. (2018) *Amer. Min., 103*, 1455–1467. [20] Saal A.E. et al. (2002) *Nature, 419*, 451–455.